First-principles investigation of atomic structures and stability of proton-exchanged layered sodium titanate

AUTHOR(S):

Mori, Masahiro; Kumagai, Yu; Matsunaga, Katsuyuki; Tanaka, Isao

CITATION:

Mori, Masahiro ...[et al]. First-principles investigation of atomic structures and stability of proton-exchanged layered sodium titanate. PHYSICAL REVIEW B 2009, 79(14): 144117.

ISSUE DATE:

2009-04

URL:

http://hdl.handle.net/2433/109877

PHYSICAL REVIEW B **79**, 144117 (2009)

First-principles investigation of atomic structures and stability of proton-exchanged layered sodium titanate

Masahiro Mori,[1] Yu Kumagai,[1] Katsuyuki Matsunaga,[1,2,*] and Isao Tanaka[1,2]
[1]*Department of Materials Science and Engineering, Kyoto University, Kyoto 606-8501, Japan*
[2]*Nanostructures Research Laboratory, Japan Fine Ceramics Center, Nagoya 456-8587, Japan*
(Received 30 January 2009; revised manuscript received 1 April 2009; published 24 April 2009)

Atomic structures and ionic substitutions in sodium titanate ($Na_{2-x}H_xTi_3O_7$), having Ti_3O_7 sheetlike layers with Na^+ and H^+ in between, were investigated by first-principles calculations. The formation energies via ion exchange of Na^+ and H^+ were analyzed by using the supercell total energies and ionic chemical potentials determined with the aid of experimental thermodynamic data. It was found that ionic substitutions of Na^+ by H^+ take place even in alkaline solution conditions as found in previous experiments. In addition, the bonding strength between the Ti_3O_7 layers tends to decrease with more Na^+ substitutions by H^+, which is related to *p*H effects on exfoliation events of Ti_3O_7 sheetlike layers from layered titanate prior to the nanotube formation.

DOI: 10.1103/PhysRevB.79.144117 PACS number(s): 61.72.−y, 77.84.Dy

I. INTRODUCTION

Recently, titanate nanotubes have drawn great scientific and industrial attention, since Kasuga *et al.* reported preparation of TiO_2-derived titanate nanotubes by an alkaline hydrothermal method.[1] The nanotube fabrication by the alkaline hydrothermal method can be easily performed by treating TiO_2 powder in a superboiled (110–150 °C) solution of concentrated NaOH (5–15 M) without any sacrificial templates. The titanate nanotubes are multiwalled scroll-type open-ended ones with a diameter of about 80 Å and a layered spacing of about 7–8 Å. These titanate nanotubes are expected that their unique structure derives numerous applications not only to photocatalysis[2–5] and catalysis,[6–9] but also to ion exchange,[10–12] Li battery,[13–15] hydrogen storage,[16,17] and even a nanoscale confinement tool[18,19] or reaction environment.[20]

Many groups have attempted to reveal a formation mechanism of the TiO_2-derived titanate nanotubes. Apparently, there is a consensus that, after breaking of chemical bonds in the starting three-dimensional TiO_2 structure by high concentrated NaOH aqueous solution, layered titanates are formed as intermediate, and then they converted into nanotubes through a Ti-O sheet folding mechanism. Sodium titanate ($Na_2Ti_3O_7$) is regarded as one of candidates for the intermediate phase (the crystal structure shown in Fig. 1). This is because this material has a crystal structure containing Ti-O layers and the chemical composition of the individual Ti-O layer (Ti_3O_7) is close to a typical Ti/O molar ratio of the TiO_2-derived titanate nanotubes (such as $H_2Ti_3O_7$). However, the nanotube formation occurs in concentrated NaOH solutions, and it is expected that Na^+ ions in this phase may be partially substituted by other ions, typically H^+, via ion exchange. Concentrations and spatial distribution of such ionic substitutions in the layered titanate will strongly affect exfoliation events of Ti_3O_7 sheets from the layered titanate prior to the sheet folding. In this regard, Zhang *et al.* and their co-workers theoretically investigated properties and the cleavage mechanism of Ti_3O_7 sheets from $H_2Ti_3O_7$ by first-principles calculations,[21–24] and discussed that the asymmetric attachment of protons on two surfaces of Ti_3O_7 sheets induces cleavage and folding of the sheets. However, they did not take into account the effect of NaOH solution for the exfoliation mechanism and the sequential nanotube formation. The NaOH-solution effect will be essential because highly concentrated NaOH solutions were commonly used for the nanotube fabrication. Moreover, according to Morgado Jr. *et al.*,[25] Na content and the degree of ion exchange by protons in titanate nanotubes are considered to play an important role for the atomic structures and thermal stability.

In this study, electronic and atomic structures of the layered titanates ($Na_{2-x}H_xTi_3O_7$, $x=0-2$) are calculated by first-principles calculations, in order to investigate the stable composition in concentrated NaOH aqueous solution. $Na_2Ti_3O_7$ and $H_2Ti_3O_7$ are used as starting structural models, and substitutions of H^+ or Na^+ ions in their structures are considered. Formation energies of the substituted layered-titanate structures are evaluated from total energies of supercells, together with chemical potentials determined under chemical equilibrium with NaOH aqueous solution. From the *p*H-dependent stability of the layered titanates and cleavage energies of Ti_3O_7 sheets, the NaOH aqueous solution effect on exfoliation of the Ti_3O_7 sheets from the layered titanate, which occurs prior to the nanotube formation, will be discussed.

II. COMPUTATIONAL METHOD

A. Electronic structure calculation and supercell

First-principles electronic structure calculations are performed by the projector augmented wave (PAW) method, implemented in VASP.[26–28] The generalized gradient approximation (GGA) is used for the exchange-correlation potential, and the GGA functional proposed by Perdew *et al.*[29] is employed. Wave functions are expanded up to a plane-wave cutoff energy of 500 eV and the Brillouin-zone integration is performed by the $2\times2\times2$ Monkhorst-Pack scheme for supercell calculations described below. The *k*-point sampling condition ensures a good accuracy of total energies for layered titanate within about 1 meV/f.u. Based on forces on atoms calculated, all atomic positions, cell parameters and

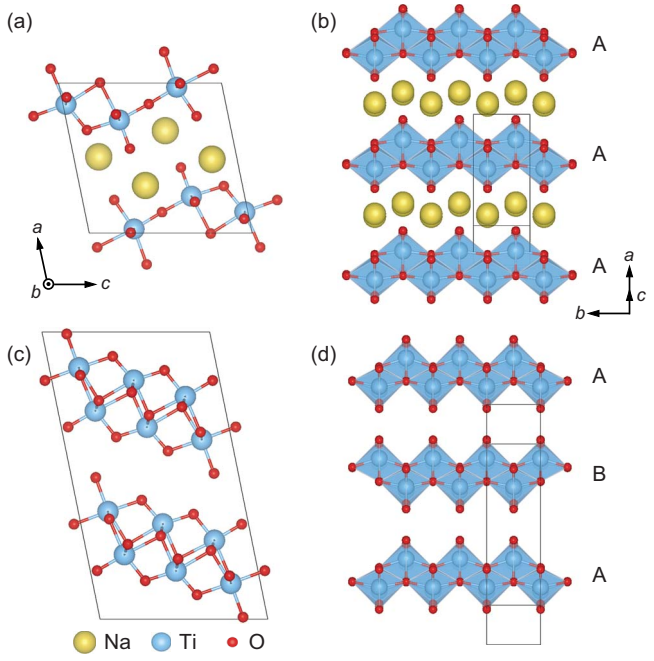

FIG. 1. (Color online) Crystal structures of $Na_2Ti_3O_7$ [(a) and (b)] and $H_2Ti_3O_7$ ((c) and (d)). (a) and (c) are viewed along the *b* axis. (b) and (d) are drawn in a particular direction, and TiO_6 octahedra are colored in blue, in order to highlight the stacking sequence of the Ti_3O_7 layers. It is noted that Feist *et al.* (Ref. 31) did not explicitly determine hydrogen locations in $H_2Ti_3O_7$ and thus no hydrogen atoms are drawn in (b) and (d).

cell shapes of unit cells and supercells are allowed to relax until their forces converge to less than 0.02 eV/Å. In the PAW potentials, electrons of $1s^1$ for H, $3s^1$ for Na, $4s^13d^3$ for Ti and $2s^22p^4$ for O are treated as valence.

In this study, crystal structures of $Na_2Ti_3O_7$ and $H_2Ti_3O_7$ are used as structural models for $Na_{2-x}H_xTi_3O_7$. These compounds can be considered as end members of the solid solution $Na_{2-x}H_xTi_3O_7$, but they have different stacking sequences of Ti_3O_7 layers, as will be discussed below. Figure 1 displays atomic structures of $Na_2Ti_3O_7$ and $H_2Ti_3O_7$. According to Andersson *et al.*[30] and Feist *et al.*,[31] $Na_2Ti_3O_7$ has a monoclinic structure (space group $P2_1/m$) and the lattice parameters of $a=8.571$ Å, $b=3.804$ Å, $c=9.135$ Å, and $\beta=101.57°$, while the monoclinic phase of $H_2Ti_3O_7$ (space group $C2/m$) has lattice parameters $a=16.025$ Å, $b=3.747$ Å, $c=9.188$ Å, $\beta=101.46°$. In both cases, TiO_6 octahedra are linked to one another along the *bc* plane by corner and edge shearing, forming the sheetlike titanium oxide (Ti-O) layers. The resultant chemical composition of the individual Ti-O layer is Ti_3O_7, which is quite similar to the Ti/O molar ratio in typical titanate nanotubes previously fabricated. It is also noted here that there is a difference in stacking sequences of the Ti_3O_7 layers along the *a* axis between the two crystal structures: one Ti_3O_7 layer in $H_2Ti_3O_7$ is relatively displaced by $b/2$ with respect to another. Therefore, the stacking sequences of the Ti_3O_7 layers can be described as ..AAAA.. and ..ABAB.. in $Na_2Ti_3O_7$ and $H_2Ti_3O_7$, respectively.

First, structural optimization of $Na_2Ti_3O_7$ and $H_2Ti_3O_7$ is conducted using supercells containing 48 atoms. In the case

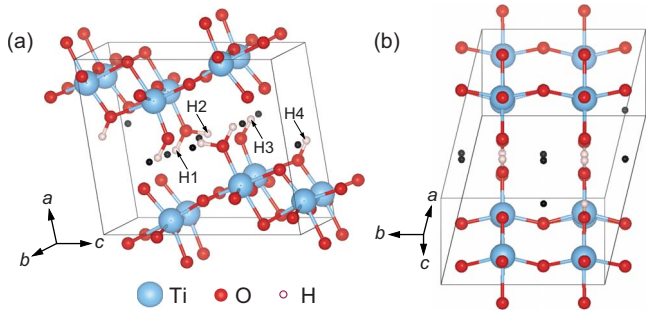

FIG. 2. (Color online) Optimized atomic structure of the $H_2Ti_3O_7$ supercell. Small black spheres indicate substitutional sites of Na^+ (see details in text).

of $Na_2Ti_3O_7$, the supercell is obtained by doubling the unit cell shown in Figs. 1(a) and 1(b) along the *b* axis. On the other hand, the $H_2Ti_3O_7$ supercell is generated by using a different cell shape from the unit cell and doubling this cell along the *b* axis (see Fig. 2), so as to make the supercell size and shape similar to the $Na_2Ti_3O_7$ case. Since, in the experiment of Feist *et al.*,[31] H^+ positions in $H_2Ti_3O_7$ were not unambiguously determined, H^+ ions are introduced in the middle of nearest neighboring O^{2-} ions in the two adjacent Ti_3O_7 layers in the present study. As can be seen in Fig. 2, however, H^+ ions in the optimized structure are no longer located in the middle of O^{2-} ions in the Ti_3O_7 layers. One H^+ is attached to O^{2-} ions bridging two TiO_6 octahedra (H4), and nonbridging O^{2-} ions tend to be bonded to one or two H^+ ions (H1–3). The O-H bond lengths are about 1.0 Å, and their bonding directions are oriented to O^{2-} ions in the adjacent Ti_3O_7 layer, which is similar to hydrogen bonding linkages as found in ice and water. It is noted here that static structure optimization in the first-principles calculations may find metastable configurations of ∠Ti-O-H angles (O-H bonding directions; see Fig. 2). In order to examine this, test calculations of the H^+ ions having slightly different ∠Ti-O-H angles from those optimized in the above manner were performed, and it was confirmed that Fig. 2 indicates the H^+ positions energetically most stable. The cell lengths and angles thus calculated are listed in Table I, which are in reasonable agreement with experiment.

Regarding the atomic structure of $H_2Ti_3O_7$, Zhang *et al.*[22] also performed the similar first-principles calculation of the titanate. They used the crystal structure of $Na_2Ti_3O_7$ by Andersson *et al.*[30] as a model, and calculated several atomic configurations of protons introduced instead of Na^+, in a different way from the present study. Therefore, test calculations with respect to the $H_2Ti_3O_7$ model by Zhang *et al.* [the energetically most favorable structure of H(1,3) in Ref. 22]

TABLE I. Calculated lattice parameters of $Na_2Ti_3O_7$ and $H_2Ti_3O_7$. For $H_2Ti_3O_7$, the values listed here are based on the original space group $C2/m$.

	a (Å)	*b* (Å)	*c* (Å)	β (deg.)
$Na_2Ti_3O_7$	8.583	3.836	9.218	101.6
$H_2Ti_3O_7$	16.188	3.797	9.281	101.5

were also carried out, and it was found, however, that the formation energy of the Zhang's model is larger by about 0.525 eV/f.u. than the present $H_2Ti_3O_7$ model based on Feist *et al.*[31]

In NaOH aqueous solutions, as often encountered in the previous experiments for titanate nanotubes, it is expected that some of Na^+ ions in $Na_2Ti_3O_7$ are replaced by H^+, depending on the solution *p*H condition, which is considered to affect atomic structures and thermal stability of titanate nanotubes.[25] In order to calculate such ion-exchanged structures of $Na_{2-x}H_xTi_3O_7$, H^+ ions are substituted for Na^+ ions in the $Na_2Ti_3O_7$ supercell (eight Na^+ ions involved in the supercell), varying the x value from 0 to 2, and the atomic positions and the cell parameters of the supercells are optimized in the manner described above. It should be noted that there are a number of possibilities for substitutional configurations of H^+ in the $Na_2Ti_3O_7$ supercell, depending on the value of x. In order to thoroughly investigate various ion-exchanged configurations, all of the possible substitutional configurations for Na^+ and H^+ in the $Na_{2-x}H_xTi_3O_7$ supercells are taken into account over the entire range of x.

The similar procedure is also applied to $H_2Ti_3O_7$ having the different stacking sequence of the Ti_3O_7 layers from $Na_2Ti_3O_7$, and H^+ ions in the $H_2Ti_3O_7$ supercell are exchanged by Na^+ ions for the $Na_{2-x}H_xTi_3O_7$ calculations with different x values. It is worth noting, however, that substituting Na^+ for H^+ in the original $H_2Ti_3O_7$ supercell results in the close proximity between the substituted Na^+ and the adjacent O^{2-} ions: the distance between oxygen in the O-H···O linkage in $H_2Ti_3O_7$ is about 2.6–2.8 Å, whereas the diameter of a Na^+ ion is about 2 Å.[32] In order to avoid such a situation, the substituted Na^+ ions are located at adjacent open spaces by being shifted by $b/4$ from the original H^+ sites (see Fig. 2). In this case, the substituted Na^+ ion has a fourfold coordination with oxygen and the average bond length of Na-O is about 2.3–2.4 Å, which is close to the local atomic coordination environment in bulk Na_2O. It can be thought, therefore, that such location of substituting Na^+ is reasonable for the $Na_{2-x}H_xTi_3O_7$ calculations based on the $H_2Ti_3O_7$ supercells. It is also noted that all substitutional configurations of Na^+ ions are considered, according to the symmetry of the calculated $H_2Ti_3O_7$ supercell (a 2_1 helical axis along b axis and a plane of mirror symmetry perpendicular to the axis). As a final note, the total number of the configurations of Na^+ and H^+ practically treated in the present calculations is 193.

B. Formation energies of $Na_{2-x}H_xTi_3O_7$

In order to search the stable composition and atomic structure of the $Na_{2-x}H_xTi_3O_7$ system in NaOH aqueous solutions, we calculated formation energies of $Na_{2-x}H_xTi_3O_7$ with different x and Na^+ (or H^+) configurations, based on the total energies of the supercells. For this purpose, it is assumed that $Na_{2-x}H_xTi_3O_7$ is formed from $Na_2Ti_3O_7$ or $H_2Ti_3O_7$ in NaOH aqueous solution. Then the following ion-exchange reaction for formation of $Na_{2-x}H_xTi_3O_7$ is considered:

$$Na_2Ti_3O_7(s) + xH^+(aq) = Na_{2-x}H_xTi_3O_7(s) + xNa^+(aq). \quad (1)$$

By using the total energies of the $Na_{2-x}H_xTi_3O_7$ supercells (E_t), the formation energy of $Na_{2-x}H_xTi_3O_7$ (ΔE_{form}), according to Eq. (1), can be given by

$$\Delta E_{form} = E_t(Na_{2-x}H_xTi_3O_7) + x\mu_{Na^+,aq} - E_t(Na_2Ti_3O_7) - x\mu_{H^+,aq}, \quad (2)$$

where $\mu_{Na^+,aq}$ and $\mu_{H^+,aq}$ indicate chemical potentials of Na^+ and H^+ in the NaOH aqueous solution. These ionic chemical potentials can be written in terms of the standard chemical potential ($\mu^\circ_{M^+,aq}$) and the ionic activity ($a_{M^+,aq}$) as

$$\mu_{M^+,aq} = \mu^\circ_{M^+,aq} + k_BT \ln a_{M^+,aq}. \quad (3)$$

In this equation, k_B is the Boltzmann constant, and T is the temperature (T=298 K throughout the present study). Then Eq. (1) can be rewritten as

$$\Delta E_{form} = E_t(Na_{2-x}H_xTi_3O_7) - E_t(Na_2Ti_3O_7) + x(\mu^\circ_{Na^+,aq} - \mu^\circ_{H^+,aq}) + 2.303xk_BT \times(\log a_{Na^+,aq} + pH). \quad (4)$$

In order to calculate ΔE_{form}, it is necessary to evaluate the third and forth terms of the right-hand side of Eq. (4). As described in our previous paper,[33–35] the third term of the standard chemical-potential difference can be obtained in terms of the standard Gibbs formation energy of Na^+ in aqueous solution (ΔG°_f) as follows:

$$\mu^\circ_{Na^+,aq} - \mu^\circ_{H^+,aq} = \Delta G^\circ_f(Na^+,aq) + \mu^\circ_{Na,s} - \frac{1}{2}\mu^\circ_{H_2,g}. \quad (5)$$

For $\Delta G^\circ_f(Na^+,aq)$, the experimental thermodynamic data at T=298 K is used in this study. The bcc solid phase of Na and the isolated H_2 molecule are separately calculated in the first-principles manner, and the total energies per atom or molecule are used to evaluate $\mu^\circ_{Na,s}$ and $\mu^\circ_{H_2,g}$. It is noted that temperature-dependent entropy and enthalpy terms were also considered for $\mu^\circ_{H_2,g}$, which was described in detail elsewhere.[33–35]

C. Activities of ionic species in concentrated NaOH aqueous solution

In order to calculate ΔE_{form}, the remaining forth term in Eq. (4) has to be prepared. In NaOH aqueous solutions, the activity of Na^+ ($a_{Na^+,aq}$) and the solution *p*H are correlated with each other. In this study, a NaOH concentration of the aqueous solution is assumed, and then the solution *p*H is evaluated in the following manner.

At a given concentration of NaOH in the solution, molalities of Na^+ ($m_{Na^+,aq}$) and OH^- ($m_{OH^-,aq}$) can be considered to be equal to each other. Also, the activity coefficients of the respective ions cannot be independently determined, and thus are generally approximated by the mean activity coefficient $\gamma_\pm(\cong\gamma_{Na^+,aq}=\gamma_{OH^-,aq})$ which is defined as

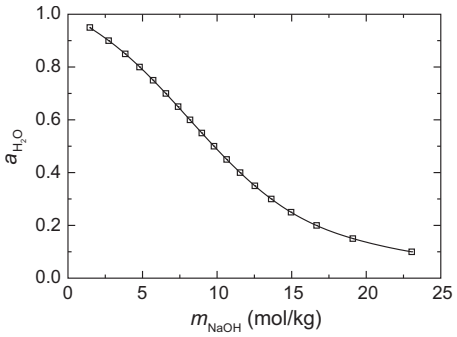

FIG. 3. Variation in water activity as a function of molality of NaOH, according to Ref. 37.

$$\gamma_{\pm} = \sqrt{\gamma_{Na^+,aq}\gamma_{OH^-,aq}}. \quad (6)$$

Since it is not straightforward to calculate the activity coefficient theoretically, the experimental value as a function of molality of NaOH is used here.[36] Then the activity of Na^+ and OH^- in the solution can be determined as follows:

$$a_{Na^+,aq} = m_{Na^+,aq}\gamma_{Na^+,aq}, \quad \text{and} \quad a_{OH^-,aq} = m_{OH^-,aq}\gamma_{OH^-,aq}. \quad (7)$$

In terms of the ionic product of water (K_w) and the water activity (a_{H_2O}), the following equation is also obtained,

$$K_w = \frac{a_{H^+,aq}a_{OH^-,aq}}{a_{H_2O}}. \quad (8)$$

From this equation, the solution pH(=$-\log a_{H^+,aq}$) can be given as

$$p\mathrm{H} = \log a_{OH^-,aq} - \log K_w - \log a_{H_2O}. \quad (9)$$

In a normal aqueous solution, the water activity a_{H_2O} is considered to be unity. However, it was experimentally reported that a_{H_2O} tends to decrease with increasing NaOH concentration.[37] The highly concentrated NaOH solutions (the pH range of more than 10, as found in the common Ti-O nanotube fabrication) are mainly considered in the present study, hence the experimental a_{H_2O} value against the NaOH content (Fig. 3) is used to evaluate the solution pH. From the values of $a_{Na^+,aq}$ and pH thus evaluated, the formation energies of $Na_{2-x}H_xTi_3O_7$ can be calculated by using Eq. (4).

III. RESULTS AND DISCUSSION

A. Atomic structures of $Na_{2-x}H_xTi_3O_7$

Figure 4 displays calculated formation energies of all possible configurations as a function of x, according to the ion-exchange reaction of Eq. (1). In this case, the solution pH is assumed to be 16, which corresponds to the NaOH concentration in solution of 10.9 mol/kg, as estimated from Fig. 3 and Eq. (9).

In the compositions of $0 \le x \le 0.75$, the most stable atomic structures have the same Ti_3O_7-layer stacking sequence as found in $Na_2Ti_3O_7$ given by Andersson *et al.*[30] ("AAAA"), while those in the range of $1 \le x \le 2$ is composed of the "ABAB" Ti_3O_7-layer stacking sequence with the one of the $H_2Ti_3O_7$ structure given by Feist *et al.*[31] For instance, Fig. 5 shows most stable calculated atomic structures for $x=1(NaHTi_3O_7)$ and $x=1.5(Na_{0.5}H_{1.5}Ti_3O_7)$. The O-H bonds between the Ti_3O_7 layers are oriented toward O^{2-} ions in the neighboring Ti_3O_7 layer.

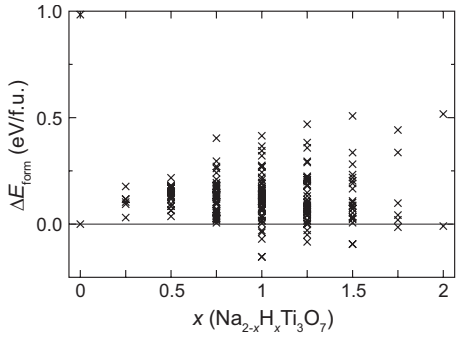

FIG. 4. Calculated formation energies of all possible atomic configurations for $Na_{2-x}H_xTi_3O_7$ as a function of x. In this case, the condition of pH=16 is assumed.

Pálinkás *et al.*[38] defined the presence of hydrogen bonds between two H_2O molecules from the O···O distance of less than 3.28 Å and the angle between the O-H bond vector and the O···O vector (∠H-O···O) of less than 20°. According to this definition, the local atomic structures of the proton in $Na_{2-x}H_xTi_3O_7$ are analyzed. Table II shows O-H bond lengths, O···O distances, and ∠H-O···O angles around the protons. Since the local bonding configurations of H^+ in $Na_{2-x}H_xTi_3O_7$ ($1 \le x$) satisfy the above definition, they are considered to play an important role for making hydrogen bonding linkages between the Ti_3O_7 layers.

B. Formation energies as a function of pH

For the most stable atomic configurations for the respective x values (Figs. 4 and 5), the dependence of their stability

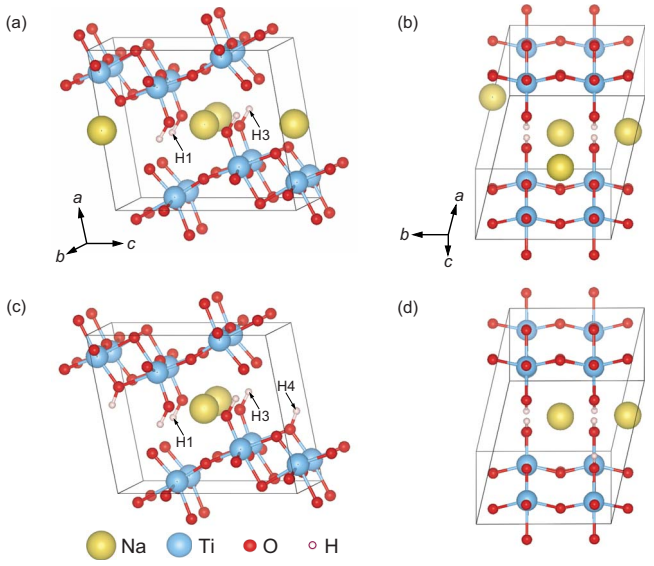

FIG. 5. (Color online) Optimized atomic structures of [(a) and (b)] $NaHTi_3O_7$ and [(c) and (d)] $Na_{0.5}H_{1.5}Ti_3O_7$.

TABLE II. Interatomic distances and bond angles around protons. The proton sites are displayed in Figs. 2 and 5.

x	Proton site	O-H length (Å)	O···O distance (Å)	∠H-O···O angle (deg.)
1	H1	1.01	2.63	7.3
	H3	1.01	2.63	7.3
1.5	H1	1.01	2.58	8.0
	H3	1.02	2.57	6.8
	H4	1.00	2.80	3.7
2	H1	1.02	2.58	0.9
	H2	1.03	2.60	0.2
	H3	1.01	2.61	2.6
	H4	1.00	2.80	5.0

on the solution pH is investigated. Figure 6 shows formation energies of $Na_{2-x}H_xTi_3O_7$ as a function of pH. As can be understood from Eq. (4), the formation energies tend to increase with rising pH, except for $x=0$. As more Na^+ ions are substituted by H^+ ions (increasing x), the gradients of the formation energy variations tend to become steeper. As a result, it can be seen that the most energetically favorable compositions are found to be $x=1(NaHTi_3O_7)$ for pH >14.9, $x=1.5(Na_{0.5}H_{1.5}Ti_3O_7)$ for $14.4<p\mathrm{H}<14.9$, and $x=2(H_2Ti_3O_7)$ for $p\mathrm{H}<14.4$. Since typical titanate-nanotube fabrication experiments used about 10 M NaOH solutions, which corresponds to the pH condition of around 16 as estimated from Eq. (9) and Fig. 3, it can be said that more than half of Na^+ ions in $Na_2Ti_3O_7$ are replaced by H^+ ions, even in the rather strong alkaline solution conditions.

It is expected that the substitutions of H^+ for Na^+ in $Na_2Ti_3O_7$ may affect interlayer bonding between the Ti_3O_7 layers, which is closely related to exfoliation of Ti_3O_7 layers from the intermediate phase prior to the Ti_3O_7-sheet folding. In order to investigate the interlayer bonding strength, therefore, works of separation (W_{sep}) between the Ti_3O_7 layers in $Na_{2-x}H_xTi_3O_7$ are calculated from total-energy differences per cross section between the $Na_{2-x}H_xTi_3O_7$ supercell and the one containing an isolated Ti_3O_7-layer slab. An isolated Ti_3O_7-layer slab is generated by simply elongating the edge length perpendicular to the Ti_3O_7 layer in the $Na_{2-x}H_xTi_3O_7$ supercell and making the two surfaces of the Ti_3O_7 layer with a vacuum layer of about 10 Å. Since Na^+ ions are present between the Ti_3O_7 layers in the $Na_{2-x}H_xTi_3O_7$ supercells, unlike H^+ strongly attached to O^{2-}, it is necessary to consider detailed attachment sites and configurations of Na^+ ions onto the surfaces of the isolated Ti_3O_7 layers, when the isolated slab supercells are generated. In this study, it is assumed that both ends of isolated Ti_3O_7 layers contain an equal number of Na^+ ions, and all possible configurations of Na^+ surface attachment are calculated. By doing this, the most stable atomic structures of the Ti_3O_7-layer slabs for the compositions $x=0$, 1, 1.5, and 2, which are observed as stable compositions, are obtained in the first-principles manner, and their total energies are used to evaluate the W_{sep} values.

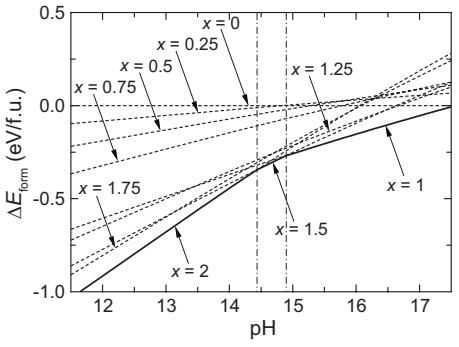

FIG. 6. Formation energies of $Na_{2-x}H_xTi_3O_7$ as a function of pH. The thick solid lines indicate the energetically most stable compositions in the respective pH ranges.

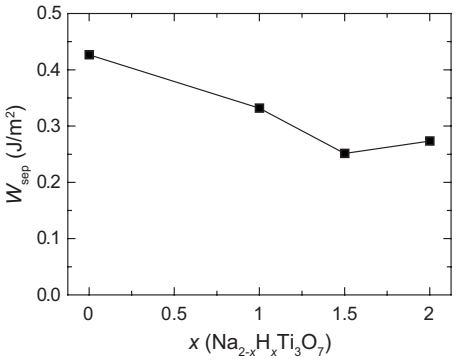

FIG. 7. Calculated works of separation of $Na_{2-x}H_xTi_3O_7$ against the composition x.

Figure 7 shows calculated works of separation against the composition x. It can be seen that the W_{sep} values tend to decrease with increasing x and those for $x\geq 1$ are smaller by more than 20%, as compared to the $Na_2Ti_3O_7$ case. Therefore, the inclusion of H^+ ions between the Ti_3O_7 layers, depending on pH, contributes to weakening the interlayer bonding strength, although H^+ ions tend to form hydrogen bonding linkages between the layers. It can be said that ionic bonding between Ti_3O_7 layers via Na^+ ions is stronger than the hydrogen bonding due to the H^+ substitutions.

Tsai *et al.*[6,39] argued the formation mechanism of titanate nanotubes from TiO_2 in the NaOH treatment of the hydrothermal process. In the proposed mechanism, the layered titanate formed as intermediate would undergo Na^+ exchange with H^+ during a post-treatment of acid washing. The smaller pH in the post-treatment promotes the nanotube formation from the layered titanate, and the material is eventually transformed into anatase in further acidic conditions. In this regard, the present calculations also showed the similar tendency that Na^+ content in $Na_{2-x}H_xTi_3O_7$ decreases by the H^+ substitution in smaller pH conditions. Even in the rather alkaline solution conditions of $p\mathrm{H}\sim 15-16$ (commonly used in previous experiments), it was found that more than a half of Na^+ ions are replaced by H^+ ions between the Ti_3O_7 layers. At the same time, the Ti_3O_7 sheets can be more easily peeled off from the layered titanate, due to the weakened interlayer strength. In other words, the Na^+ content is responsible for the chemical stability of the layered-titanate structure $Na_{2-x}H_xTi_3O_7$, which is consistent with the argument by Morgado Jr. *et al.*[25]

IV. SUMMARY

First-principles calculations were performed for $Na_{2-x}H_xTi_3O_7$, to investigate the stable atomic structures when the compounds equilibrate with concentrated NaOH aqueous solutions. The formation energies via ion exchange with Na^+ and H^+ were analyzed by using the supercell total energies and the ionic chemical potentials determined from a combination of first-principles results and experimental thermodynamic data. It was found that Na^+ content in $Na_{2-x}H_xTi_3O_7$ decreases with decreasing *p*H, and yet ionic substitutions by protons take place even in rather alkaline conditions employed in previous experiments. In addition, the interlayer bonding strength between the Ti_3O_7 layers tends to decrease with more substitutions of Na^+ ions by H^+ ions, which is related to *p*H effects on exfoliation events of Ti_3O_7 sheetlike layers from layered titanate prior to the nanotube formation.

ACKNOWLEDGMENTS

This study was supported by Grant-in-Aid for Scientific Research on Priority Areas "Nano Materials Science for Atomic Scale Modification 474" from the Ministry of Education, Culture, Sports, Science and Technology (MEXT) of Japan, and was also partly supported by a research grant from The Murata Science Foundation.

*Author to whom correspondence should be addressed; k.matsunaga@materials.mbox.media.kyoto-u.ac.jp

[1] T. Kasuga, M. Hiramatsu, A. Hosono, T. Sekino, and K. Niihara, Langmuir **14**, 3160 (1998).
[2] M. Adachi, Y. Murata, M. Harada, and S. Yoshikawa, Chem. Lett. **29**, 942 (2000).
[3] A. Nakahira, W. Kato, M. Tamai, T. Isshiki, K. Nishio, and H. Aritani, J. Mater. Sci. **39**, 4239 (2004).
[4] M. Zhang, Z. Jin, J. Zhang, X. Guo, J. Yang, W. Li, X. Wang, and Z. Zhang, J. Mol. Catal. A: Chem **217**, 203 (2004).
[5] H. Y. Zhu, Y. Lan, X. P. Gao, S. P. Ringer, Z. F. Zheng, D. Y. Song, and J. C. Zhao, J. Am. Chem. Soc. **127**, 6730 (2005).
[6] C.-C. Tsai and H. Teng, Chem. Mater. **16**, 4352 (2004).
[7] T. Akita, M. Okumura, K. Tanaka, K. Ohkuma, M. Kohyama, T. Koyanagi, M. Date, S. Tsubota, and M. Haruta, Surf. Interface Anal. **37**, 265 (2005).
[8] D. V. Bavykin, A. A. Lapkin, P. K. Plucinski, J. M. Friedrich, and F. C. Walsh, J. Catal. **235**, 10 (2005).
[9] P. Umek, P. Cevc, A. Jesih, A. Gloter, C. P. Ewels, and D. Arčon, Chem. Mater. **17**, 5945 (2005).
[10] X. Sun and Y. Li, Chem.-Eur. J. **9**, 2229 (2003).
[11] R. Ma, T. Sasaki, and Y. Bando, Chem. Commun. (Cambridge) **7**, 948 (2005).
[12] D. V. Bavykin and F. C. Walsh, J. Phys. Chem. C **111**, 14644 (2007).
[13] Y.-K. Zhou, L. Cao, F.-B. Zhang, B.-L. He, and H.-L. Li, J. Electrochem. Soc. **150**, A1246 (2003).
[14] L. Kavan, M. Kalbáč, M. Zukalová, I. Exnar, V. Lorenzen, R. Nesper, and M. Graetzel, Chem. Mater. **16**, 477 (2004).
[15] J. Li, Z. Tang, and Z. Zhang, Electrochem. Commun. **7**, 62 (2005).
[16] S. H. Lim, J. Luo, Z. Zhong, W. Ji, and J. Lin, Inorg. Chem. **44**, 4124 (2005).
[17] D. V. Bavykin, A. A. Lapkin, P. K. Plucinski, J. M. Friedrich, and F. C. Walsh, J. Phys. Chem. B **109**, 19422 (2005).
[18] M. Volel, M. Armand, W. Gorecki, and M.-L. Saboungi, Chem. Mater. **17**, 2028 (2005).
[19] X.-P. Tang, J.-C. Wnag, L. W. Cary, A. Kleinhammes, and Y. Wu, J. Am. Chem. Soc. **127**, 9255 (2005).
[20] A. Kleinhammes, G. W. Wagner, H. Kulkarni, Y. Jia, Q. Zhang, L.-C. Qin, and Y. Wu, Chem. Phys. Lett. **411**, 81 (2005).
[21] S. Zhang, L.-M. Peng, Q. Chen, G. H. Du, G. Dawson, and W. Z. Zhou, Phys. Rev. Lett. **91**, 256103 (2003).
[22] S. Zhang, Q. Chen, and L.-M. Peng, Phys. Rev. B **71**, 014104 (2005).
[23] X. G. Xu, X. Ding, Q. Chen, and L.-M. Peng, Phys. Rev. B **73**, 165403 (2006).
[24] X. G. Xu, X. Ding, Q. Chen, and L.-M. Peng, Phys. Rev. B **75**, 035423 (2007).
[25] E. Morgado, Jr., M. A. S. de Abreu, O. R. C. Pravia, B. A. Marinkovic, P. M. Jardim, F. C. Rizzo, and A. S. Araújo, Solid State Sci. **8**, 888 (2006).
[26] P. E. Blochl, Phys. Rev. B **50**, 17953 (1994).
[27] G. Kresse and J. Furthmüller, Phys. Rev. B **54**, 11169 (1996).
[28] G. Kresse and D. Joubert, Phys. Rev. B **59**, 1758 (1999).
[29] J. P. Perdew, K. Burke, and M. Ernzerhof, Phys. Rev. Lett. **77**, 3865 (1996).
[30] S. Andersson and A. D. Wadsley, Acta Crystallogr. **14**, 1245 (1961).
[31] T. P. Feist and P. K. Davies, J. Solid State Chem. **101**, 275 (1992).
[32] R. D. Shannon, Acta Crystallogr. A **32**, 751 (1976).
[33] K. Matsunaga, Phys. Rev. B **77**, 104106 (2008).
[34] K. Matsunaga, J. Chem. Phys. **128**, 245101 (2008).
[35] K. Matsunaga, H. Inamori, and H. Murata, Phys. Rev. B **78**, 094101 (2008).
[36] W. J. Hamer and Y.-C. Wu, J. Phys. Chem. Ref. Data **1**, 1047 (1972).
[37] R. A. Robinson and R. M. Stokes, *Electrolyte Solutions*, 2nd ed. (Butterworths, London, 1968).
[38] G. Pálinkás, P. Bopp, G. Jancsó, and K. Heinzinger, Z. Naturforsch. C **39a**, 179 (1984).
[39] C.-C. Tsai and H. Teng, Chem. Mater. **18**, 367 (2006).